

# The role of edge channel equilibration for the $R_{xx}$ - peak height of the integer quantum Hall effect

**J Oswald**

Institute of Physics, University of Leoben  
Franz Josef Str. 18, A-8700 Leoben, Austria  
e-mail: oswald@unileoben.ac.at

**Abstract.** A network model for magneto transport in the quantum Hall regime of a 2D electron system is presented. It is used for a systematic numerical study of the role of edge channel equilibration for the  $R_{xx}$  peak value and its dependence on sample geometry. It is shown that the voltage probes are in general not current-less and that one has to expect significant departures from a simple scaling with sample geometry.

## 1. Introduction

While the plateau values of the integer quantum Hall effect (IQHE) can be well explained by the edge channel (EC) pictures in terms of the Landauer-Büttiker (LB) formalism, the transition regime between plateaus is not accessible by this formalism. In the transition regime local quantities like  $\sigma_{xx}$  or  $\rho_{xx}$  are frequently used for characterizing the sample properties. It is not the purpose of this paper to discuss the validity of such quantities from the theoretical point of view. By using geometry dependent numerical simulations of  $R_{xx}$  it will be shown that the peak values of  $R_{xx}$  in general will not follow a simple scaling with the sample geometry like for a classical ohmic resistor. As a consequence, the extraction of geometry independent local quantities like  $\sigma_{xx}$  or  $\rho_{xx}$  is questionable. The major parameter in this context is the equilibration length  $L_{eq}$  between edge channels (EC) and bulk, which is controlled by the slope of the electrostatic potential at the sample edge. By varying this parameter a continuous transition between a regime of weak equilibration ( $L_{eq}$  much larger than the sample length  $L$ ) and very strong equilibration ( $L_{eq} \ll L$ ) can be performed. In general the equilibration length depends also on the magnetic field at which the investigated plateau transition occurs and also on whether or not the equilibration occurs between two spin states of the same Landau level (LL). However, it is not possible to cover all different cases and variations within a single paper, which anyway is the first attempt of such a numerical study. Therefore the calculations in this paper are restricted to the  $\nu = 2 \rightarrow 1$  plateau transition for a 2DES with  $n = 4 \times 10^{11} \text{ cm}^{-2}$ . For a real sample this would correspond to a transition between the 2 spin levels of the lowest LL, for which a quite short equilibration length can be expected. However, for studying the basic behavior of the sample in terms of  $L_{eq}$  this is not important at this stage of the investigations. The obtained general trends can be associated also with transitions between other plateaus. Therefore, as a simplification a

fully developed spin splitting is assumed. Investigations of transitions between other plateaus and the role of spin splitting is the topic of future work.

## 2. The network model

For the numerical simulations a network model is used, which is presented in detail in Ref. 1. Roughly speaking, this network consists of a system of interconnected ‘elementary’ QHE samples with each having a single EC pair.

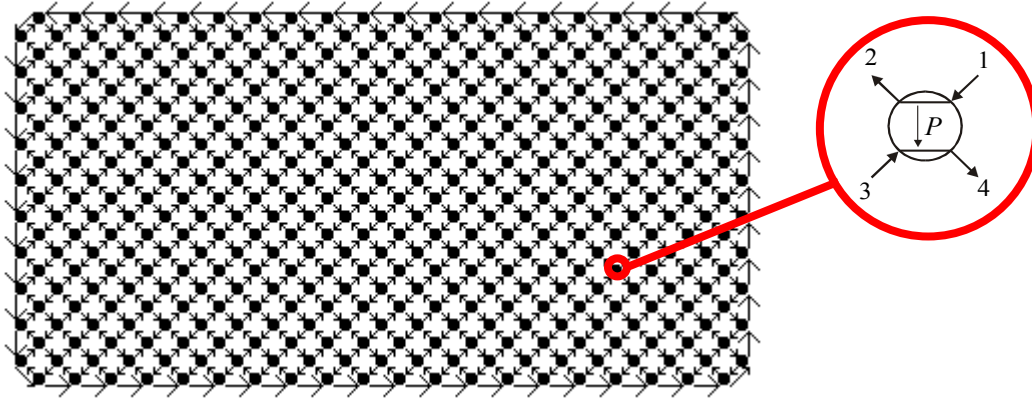


**Figure 1.** Basic network: Each node consists of 2 incoming and 2 outgoing channels and the coupling is described as a back scattering process in the edge channel picture. In this context the nodes appear like ‘elementary’ QHE samples.

All involved LLs are represented separately by such a network so that the complete system consists of some sort of multi layer network and all these layers contribute to transport in parallel. For the nodes of the network the coupling between the incoming and outgoing channels in terms of a back scattering function  $P$  is described by using  $\mu_2 = (\mu_1 + P\mu_3) / (1 + P)$  and  $\mu_4 = (\mu_3 + P\mu_1) / (1 + P)$ . This coupling is considered locally by introducing a local filling factor in the back scattering function  $P$  like  $P_j(x, y) = \exp(-v_j(x, y)/v_o(T))$ . In this way we have the possibility to introduce a lateral density variation like achieved experimentally by the shaping of the sample. The location of the node in the x-y-plane is represented by  $(x, y)$  and  $j$  is the Landau level index. Therefore  $v_j(x, y)$  is the local filling factor relative to half filling of the  $j^{\text{th}}$  LL of the node at the location  $(x, y)$  and  $v_o(T)$  is a constant parameter. The shaping of the sample can be done by distributing the proper lateral carrier density profile over the network and the corresponding filling factor needed in the coupling functions is calculated for the actual magnetic field. By use of the above equations for all nodes the network is completely determined and can be solved numerically by an iteration procedure [1].

Fig.2 provides a color representation of the bare electrostatic sample potential which defines the geometrical shape of the sample on the network. The grid points are colored according to the bare potential and the connecting channels in-between the colored grid points are plotted in gray. From the bare electrostatic potential the carrier distribution is calculated self consistently by using Fermi statistics for the occupation of the LLs and including also the feed back of the carriers on the potential. The bottom of the bare electrostatic potential is represented in blue and defines the shape of the sample where the bulk carrier density is achieved. In this way any sample layout can be numerically

shaped. After attaching contacts to the voltage probes and applying current input contacts the net work is solved and  $R_{xx}$  and  $R_{xy}$  can be calculated at different magnetic fields.

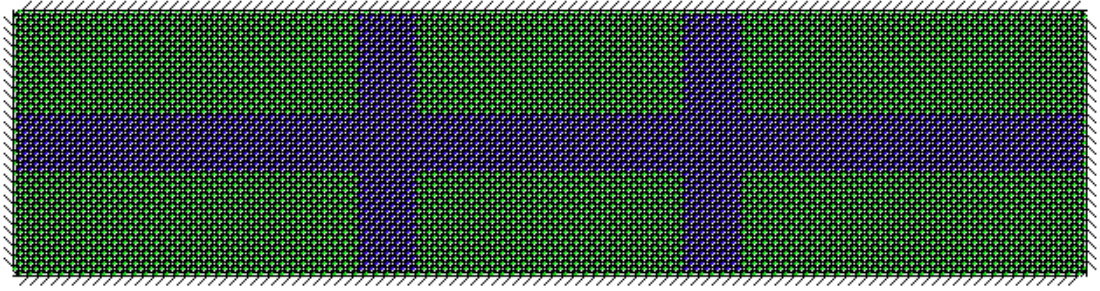


**Figure 2.** Sample layout as it appears on the network. Depending on the geometry the grid size is up to 260 x 200 grid periods. The blue area marks the regions of zero electrostatic potential where the full bulk carrier density will be achieved. The slope of the edge potential and the single arrows of the channels cannot be resolved from this representation

In Ref. 1 the different layers (LLs) of the network have been interconnected at the metallic contacts only. This means that there has been assumed to exist no equilibration outside the metallic contacts (infinite  $L_{eq}$ ). It is quite remarkable that even for that extreme assumption quite a number of experimental results have been successfully reproduced by the model[1]. For the purpose of this paper the network model has to be extended by equilibration between ECs and bulk and therefore this additional feature will now be addressed in more detail.

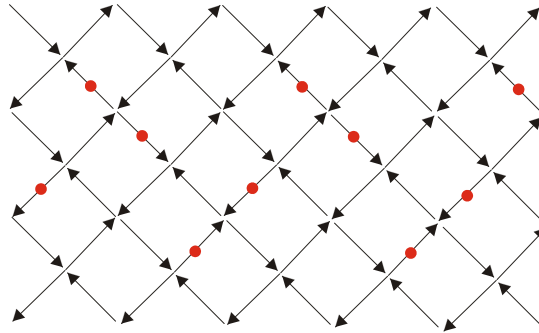


**Figure 3.** Channel scheme of the network for a single LL. Each node consists of 2 incoming and 2 outgoing channels and therefore each channel is part of a clock and a counter clock wise loop. The red dots mark the channels, which are chosen to equilibrate with the equivalent channels of the parallel layers of all the other LLs. All layers for all LLs look exactly the same and are positioned on top of each other.

Equilibration between ECs or an EC and bulk means consequently also equilibration between the associated LLs. Considering this fact we can say that for all LLs there exists only one quasi Fermi level. However, this quasi Fermi level may vary laterally due to local deviations from thermal equilibrium such as e.g. caused by current flow. The network, as explained in Ref. 1, describes the lateral distributions of the transmitted potentials through the sample and therefore, at the same time, represents the lateral variation of the quasi Fermi level. Since there should be only one local quasi Fermi level

at the same location, this means that all layers of the network, which are associated with the different involved LLs, have to carry exactly the same lateral potential profile. This means finally that between the different layers of the network also a “vertical” interconnection has to be implemented also outside the metallic contacts, which is not yet the case in Ref. 1. In order to realize this vertical interconnection we have to look for the smallest element of the network. For this purpose the network is redrawn in Fig.3 and shows the channel scheme of the network for a single LL in more detail.

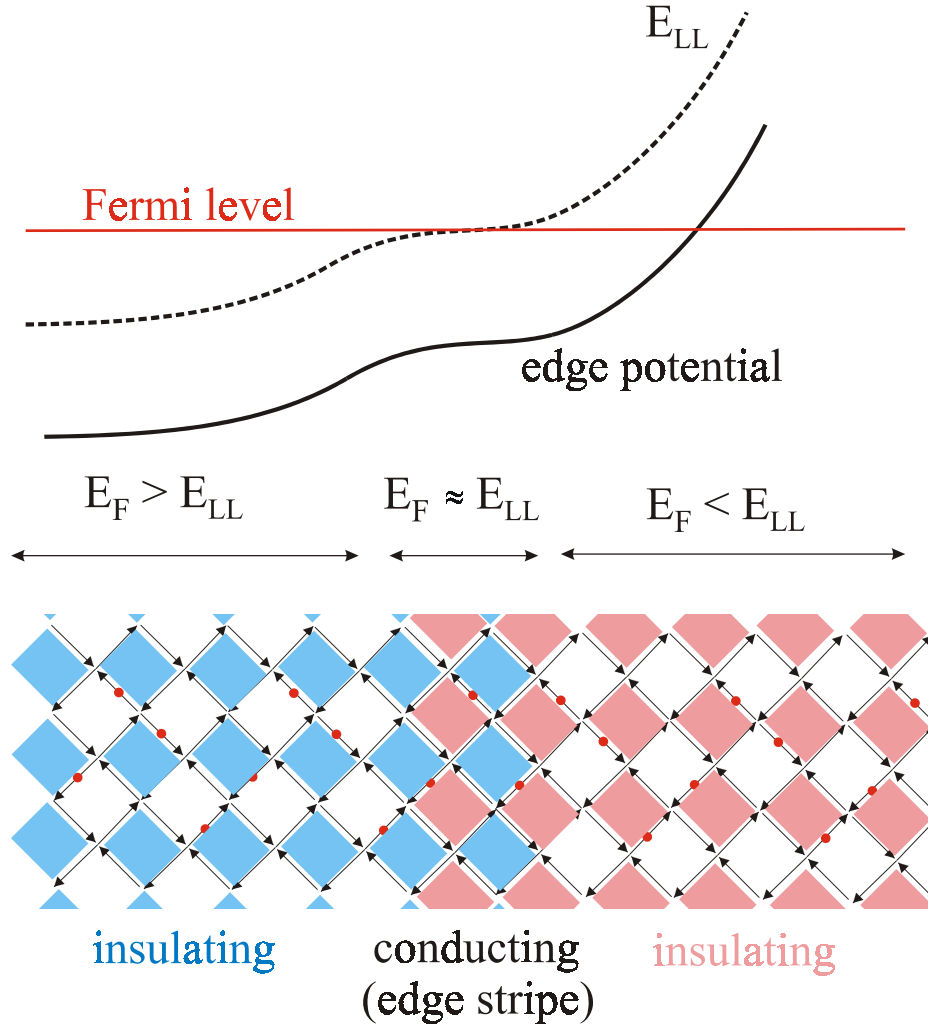


**Figure 4.** Behavior of the network at the sample edge: The upper part shows schematically the edge potential and one LL which crosses the Fermi level. The lower part shows the associated network. On the left and right of the crossing isolated loops are formed (blue means clock wise loops and red counter clock wise loops). Only in the crossing region both types of loops get interconnected and thus form conducting (edge-) stripes. These stripes are located on plateaus formed by the electrostatic edge potential [2].

Depending whether the Fermi level is above or below the center of the LL, the resulting coupling between incoming and outgoing channels forms either clock or counter clock directed loops. However, both cases create isolated loops and do not allow transport

across the network. Only if the Fermi level is close to the center of the LL each incoming channel couples to both outgoing channels so that both types of loops are activated at the same time. In this regime transport through the network is possible. This can be the case in the bulk region if we have a half filled top LL or in stripes close to the edge, where the Fermi level crosses the center of LLs (see Fig.4). In this way edge and bulk transport is described by the same network.

It is interesting to note that in case of an edge stripe the network provides directed transmission even though all directions of channels contribute in the stripe region. The direction of transmission just depends on the direction of the edge potential slope. In this way dissipation-less quantized transmission is provided even if the width of the edge stripe exceeds several grid periods of the network. This is in full agreement with experiments for investigating the width of the edge stripes, which show that edge stripes can get almost macroscopically wide (several 100 nm) without losing their 1D quantization of transport [3].

The single loops can be considered as the smallest elements of the network. For a local equilibration between different LLs all equivalent loops of the different layers (belonging to the different LLs) have to equilibrate. Technically this is done by equilibrating (averaging) ‘vertically’ the transmitted potentials of all the channels in the different layers marked with a red spot in Fig.3. Since each channel is shared by two opposite directed loops, not all of the channels have to be equilibrated. One possible scheme of choosing channels for equilibration is shown in Fig.3 and one can see that each loop, regardless clock or counter clock wise, passes exactly one red dot. As already explained in context with Fig.4, one edge stripe is formed by one LL at a position near the edge where the filling factor of this LL gets close to 0.5. If two such edge stripes (or the inner most edge stripe and the conducting bulk region) are getting closer than about 2 grid periods, the ‘vertical’ coupling between the layers of the network leads automatically also to a strong ‘horizontal’ coupling (equilibration) between these edge stripes (or the inner most edge stripe and the bulk region). If the distance increases to more than 2 grid periods this coupling decreases exponentially. In this context the loop size, which corresponds to the grid period, can be associated with the magnetic length in a real sample, where tunneling between edge channels becomes strong if their distance gets comparable to the magnetic length [2].

For the numerical studies 3 different strengths of equilibration are used: A rather weak equilibration in the network is obtained, if the bare electrostatic edge potential rises up to 500 mV within 10GP (grid periods) and this results in an equilibration length of  $L_{eq} = 240\text{GP}$ . Increasing the slope of the edge potential some what (620 mV within 10GP) we get  $L_{eq} = 72\text{ GP}$ . Increasing the slope further (500mV within 3 GP, which is already close to a step potential), we get a much stronger equilibration which results in  $L_{eq} = 10\text{ GP}$ . The shape of the bare electrostatic edge potential is chosen to be parabolic. However, the self consistent occupation with carriers creates strong deviations from the parabolic shape and forms the well known plateaus in the electrostatic edge potential at the position of the edge stripes[2]. In contrast to the authors of Ref. 2 the calculation of the self consistent edge potential is also done numerically by using some sort of ‘local capacitance’ which is charged by the carriers. This approach is alternative to Ref. 2 and will be published else where. However, the results are the same and therefore also the results Ref. 2 can be used for understanding the effect of these ‘edge plateaus’: Their major effect is that their existence demands a larger slope of potential variation from one edge potential plateau to the next within a very short distance. This results in the effect, that the region between the edge stripes gets ‘squeezed’ and in this way enhances

equilibration. The same mechanism is described by the numerical approach within the network. The details in this context will be published elsewhere.

### 3. Results and discussion

In order to investigate the role of equilibration and the role of sample geometry for the  $R_{xx}$  peak values, a systematic variation of the geometry is done at 3 different strengths of equilibration. The typical sample layout and the variation range of the parameters are given in the Fig.5 below. All lengths are given in grid periods (GP) and can be considered as arbitrary units. However, just the relation between the different lengths is important for the sample properties.

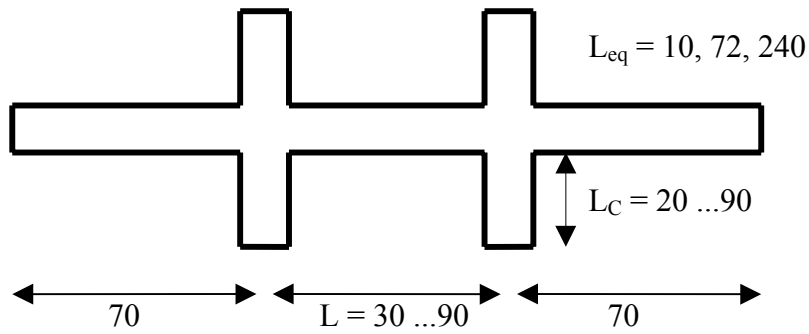


**Figure 5.** Schematic sample layout: The length scales are measured in grid periods (GP) of the network, the width of the Hall bar and the contact arms is kept fixed at 11 GP

Fig 6 below shows a typical result of a network simulation in the transition regime between QHE plateaus. The whole network is shown but in contrast to Fig.2 now the connecting channels between the grid points are colored according to their potential which they transmit (this must not be confused with the electrostatic potential of Fig.2). The color distribution of Fig.6 represents the transmitted potential of the channels and therefore is the lateral variation of the quasi Fermi level. This potential distribution can be probed by attaching contacts. As already given in the caption of Fig.6 there can be seen a weak equilibration between the EC and the bulk.



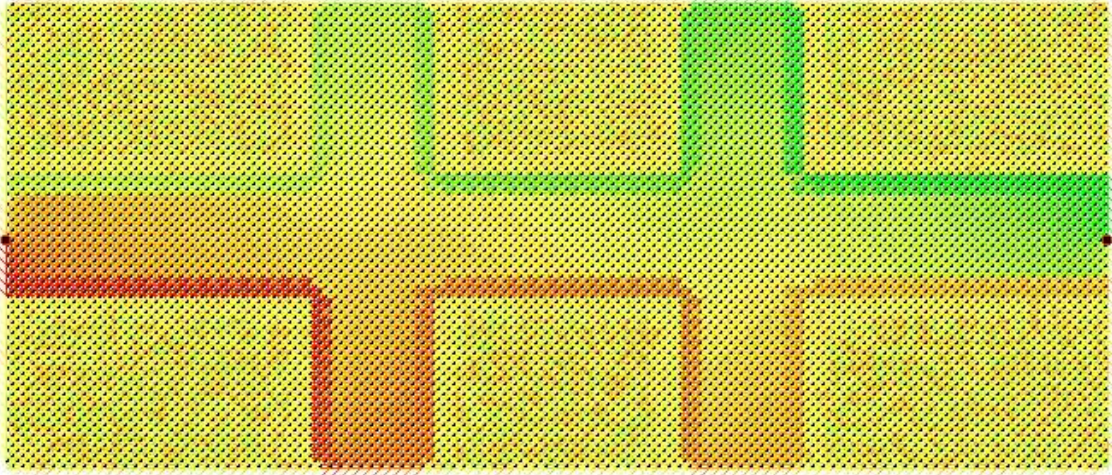


**Figure 6.** Typical solution of the network in color representation: The contours of the sample can be seen from the edge stripes. In this case there is only weak equilibration between edge and bulk, except at the end of the contact arms, where there are metallic contacts. The equilibration between edge channel and bulk leads to a gradual change of the edge channel potential. This is seen as gradual color change starting with deep red on the left and deep green on the right, where the current supply contact are located. The bulk potential distribution is not so well represented by the colors and can be seen much better in the 3D plot of Fig.7.

Before presenting the results of studying the geometry dependence also a 3D representation of the laterally transmitted potentials within a Hall bar sample with long contact arms should be shown for the 3 different values for  $L_{eq}$  in use. Fig.7 shows the case of weak equilibration, which means  $L_{eq} = 240 \text{ GP} > L$  and corresponds to the situation shown also in Fig.6. The ‘potential walls’ on the right correspond to the edge stripes, which maintain nearly constant potential. The bulk potential is embedded between the edge potentials and the large potential step between them indicates weak equilibration. The Hall voltage between both sides of the sample together with the strong equilibration between bulk and edge directly at the metallic contact (at the end of the voltage probes) causes an ohmic current in the contact arms. This current in the voltage probes leads to an almost linear voltage drop. From this one can see that opposite to the expectations from a classical 4-terminal measurement the voltage probes may not be current-less ! Fig.8 shows the same sample at intermediate equilibration ( $L_{eq} = 72 \text{ GP} \approx L$ ). In this case we can see that equilibration between edge and bulk within the voltage probes is almost completed before arriving at the metallic contacts at the end. However, as one can see there is still significant penetration of current into the contact leads. Fig.9 finally shows the same sample once more but for strong equilibration ( $L_{eq} = 10 \text{ GP} < L$ ). In this case equilibration is almost completed already within the Hall bar and therefore no current is present in the contact leads. In this case the voltage probes perform like expected for a ‘classical’ 4-terminal measurement.

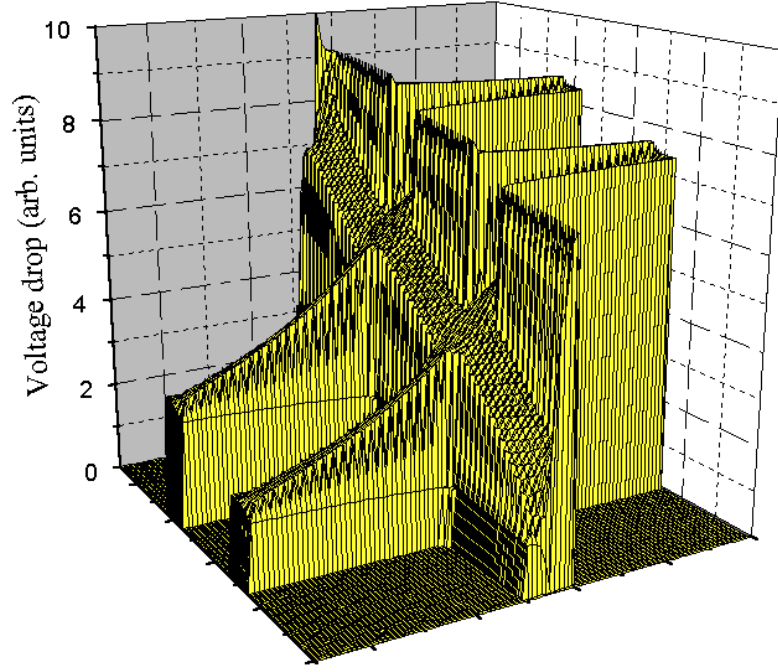


**Figure 7.** 3D plot of a typical network solution for the lateral variation of the quasi Fermi level for a Hall bar sample with long contact arms and weak equilibration. The length of the contact arms is 90 GP and the length between contacts is 70 GP. The equilibration length is  $L_{eq} = 240$  GP.

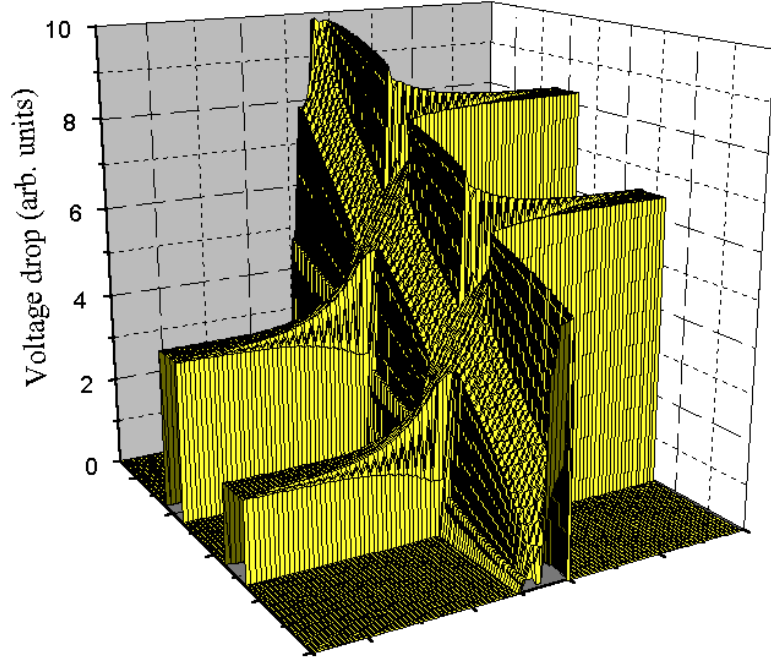


**Figure 8.** Same as Fig.7 but at intermediate equilibration, which means that  $L \sim L_{eq} = 72$  GP. In this case one can see that the equilibration along the edge now causes a slope in the edge potential along the Hall bar. In the contact arms the equilibration between edge and bulk is almost completed before arriving at the metallic contact at the end. However, at length scales less than the equilibration length there is still current in the contact arms.



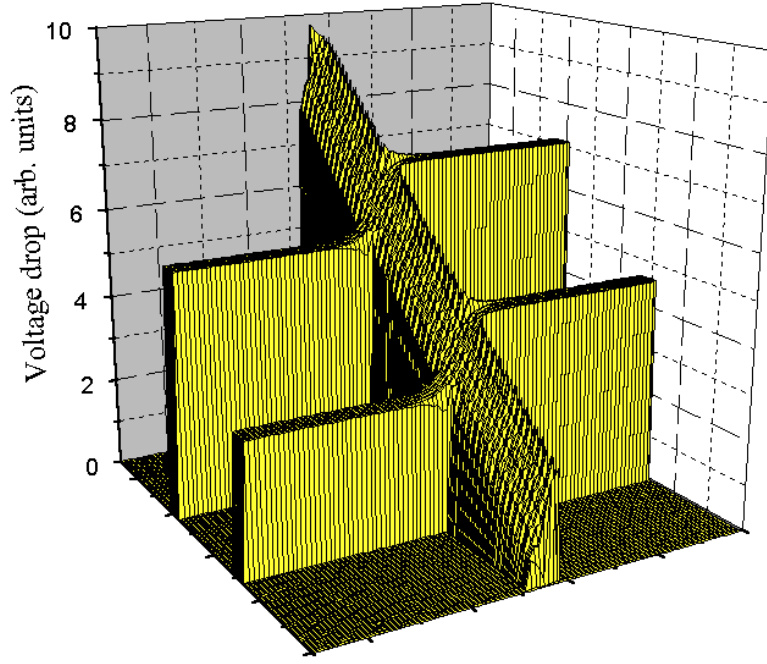


**Figure 9.** Same as Fig. 7 and Fig.8, but with strong equilibration. In this case  $L_{eq} = 10$  GP and thus, significantly shorter than  $L$  and  $L_C$ . Now we get an almost “classical” behavior of the contact arms, which means that they act as pure voltage probes like required by a 4-terminal measurement.

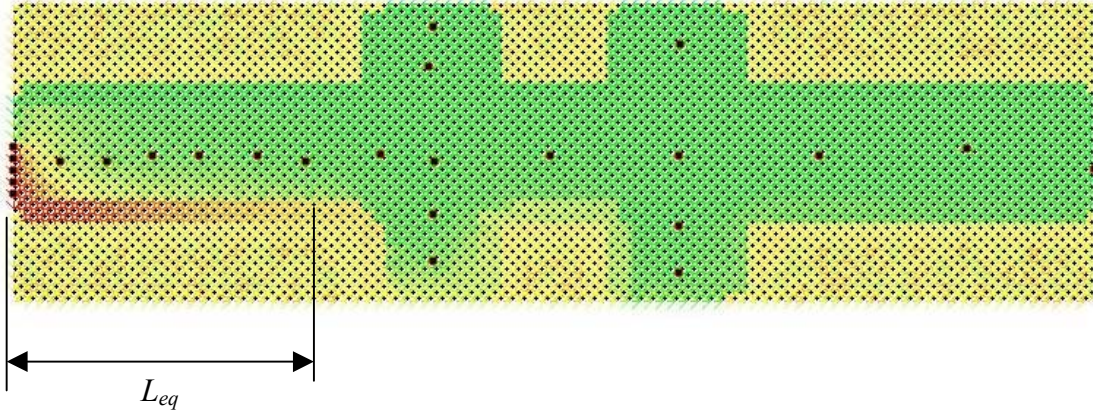


**Figure 10.** Structure for the determination of the equilibration length  $L_{eq}$ .: The bulk region is kept a low potential by applying inner contacts all over the sample structure and all are set to the same potential. The edge on the left side is supplied with the high potential by a series of contacts. After solving the network,  $L_{eq}$  can be obtained like indicated. The edge channel can be identified by the red stripe which vanishes over the distance indicating gradual equilibration.

The equilibration lengths, as given for the different sample configurations have to be determined independently by a special test geometry like shown in Fig. 10. This is done by taking the Hall geometry like used for the numerical studies, but keeping the bulk potential laterally constant at one potential while supplying the edge with a different potential. The lateral development of the edge potential is analyzed and we define  $L_{eq}$  as the distance over which the edge channel approaches half of the bulk potential (the typical lateral variation in this case is an exponential decrease). In contrast to the “visual”

representation of  $L_{eq}$  in Fig.10, a more accurate analysis was done by inspecting directly the numbers on the data files.

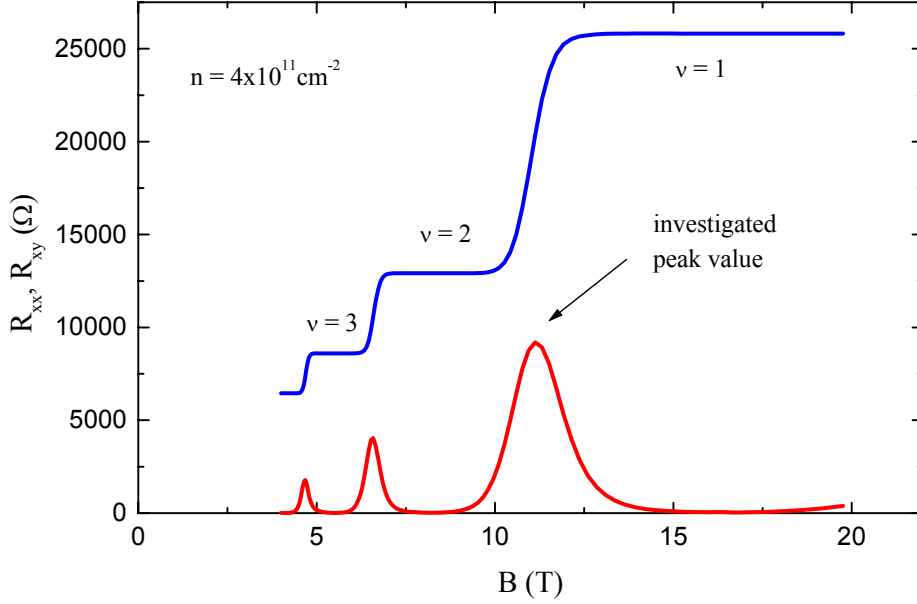


**Figure 11.** Typical result for  $R_{xx}$  and  $R_{xy}$  obtained from the network model

Fig.11 shows  $R_{xx}$  and  $R_{xy}$  over a wide range of the magnetic field and the well known behavior is obtained. For the geometry dependence at different equilibration lengths only a smaller magnetic field range around the  $\nu = 2 \rightarrow 1$  peak was used and the peak values have been extracted and plotted in the diagrams of Fig. 12 –14.

Reconsidering Figs. 7-8, we have to expect that the current flow in the voltage probes should have an impact on the ‘measured’  $R_{xx}$ , which consequently should lead to a deviation from a pure geometrical scaling behavior. In order to investigate this effect, a systematic variation of the length  $L$  is done and the peak value of  $R_{xx}$  is plotted versus  $L$  for 3 equilibration lengths  $L_{eq}$ . Fig.12a is the case with the weakest equilibration: As can be seen from the linear fit, there is a linear dependence on the sample length  $L$ , but this linear function is offset by a certain amount of about  $3000\Omega$ . If one would use the length and width ratio in order to obtain geometry independent values in terms of  $\rho_{xx}$  or  $\sigma_{xx}$ , the extracted values would vary between samples with different lengths (which makes not much sense, of course). Looking at Fig.12b at intermediate equilibration, there is again a linear dependence and the offset is less than before (about  $1000\Omega$ ). In this case the behavior is already much closer to the simple behavior of an ohmic resistor. For strong equilibration as shown in Fig.12c there is nearly no offset of the linear dependence anymore. If one looks carefully, just a negligible small negative offset can be found.

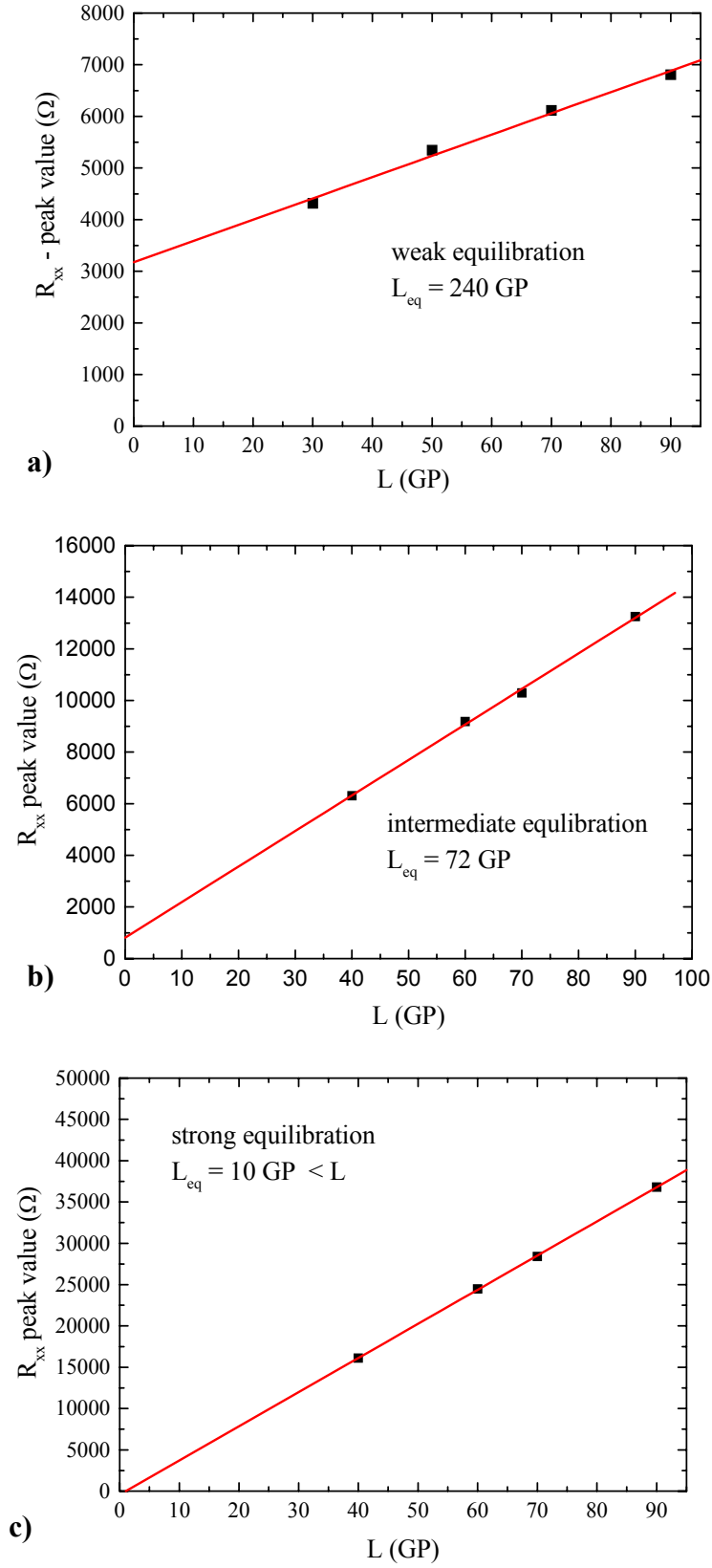


**Figure 12.** Peak value of  $R_{xx}$  at 3 different equilibration levels as a function of  $L$ . The length is measured in grid periods (GP) of the network. Mind the different  $R_{xx}$  scales in the plots.

In order to explain this strange behavior, another trend is investigated: Fig.13 shows the  $R_{xx}$  peak height as a function of the length of the voltage probes  $L_C$  for the case of weak equilibration ( $L_{eq} = 240$  GP). It clearly shows a decrease of  $R_{xx}$  by increasing  $L_C$ . This is a pure non-local behavior and is definitely in conflict with the demands of a 4-terminal measurement. However, the behavior can be easily understood by looking back to Fig.7.: Here we see, that most of the equilibration happens at the metallic contacts, remote from the classical current path. As already mentioned above, this leads to an ohmic (dissipative) current in the voltage probe, which is basically determined by the Hall voltage and the resistance of the contact arms. This causes an additional dissipation which must show up as an additional longitudinal resistance adding to the  $R_{xx}$  of the pure Hall bar. This explanation is supported by Fig.13 for the following reason: For long voltage probes these have a larger ohmic resistance and only less current flows in the voltage probes and thus less additional non-local dissipation appears. Therefore a decrease of  $R_{xx}$  results from increasing the length of the voltage probe  $L_C$ . This effect is partly suppressed at in the case of intermediate equilibration ( $L_{eq} = 72$  GP). In this case a part of the equilibration happens already on the way along the Hall bar. At the same time the dependence on the length of the voltage probes disappears if the length  $L_C$  is getting larger than the equilibration length (not shown). For strong equilibration ( $L_{eq} = 10$  GP) almost full equilibration is achieved already in the Hall bar and nothing is left to equilibrate for the contacts. It is even opposite: In the case of very strong equilibration already in the Hall bar the region where the contact leads enter the Hall bar even act as a region of reduced equilibration (missing edges) and therefore leads to a small negative offset of the  $R_{xx}$  versus  $L$  dependence.

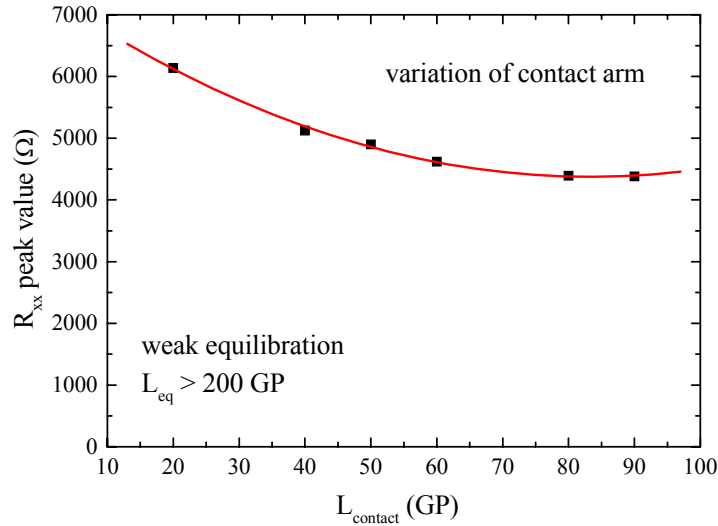


**Figure 13.** Peak value of  $R_{xx}$  versus contact arm length  $L_C$  at weak equilibration at fixed length and width of the Hall bar. The red line is just to guide the eye.

Thinking about a possible experimental verification of such an offset of the linear  $R_{xx}$  dependence it should be said, that the usual approach of having a series of voltage probes on a single sample for measuring the length dependence cannot be used. The reason is

that the changing number of “unused” voltage probes on the Hall bar will simulate a zero offset behavior. The experiment would have to be performed on different parts of a sample or on different samples with different distance between voltage probes but without unused contacts in between.

Considering the question of non-ideal contacts, the following gets quite clear from considering Fig. 8-9: If the contact leads are significantly longer than the equilibration length, any loss of edge channels before reaching the metallic contacts does not influence the results because of the equilibration in the contact leads. Numerical studies on possible experimental consequences of non-ideal contacts are in progress and will be published else where.

#### 4. Summary

A numerical study of the role of edge channel equilibration for the  $R_{xx}$  peak value and it's geometry dependence has been presented. It has been shown that the voltage probes are in principle not current-less and that one has to expect significant departures from a simple scaling with geometry. Although a linear dependence on the length of the Hall bar  $L$  is found, an offset value of the linear function, may occur. This offset value results from additional equilibration at the metallic contacts of the voltage probes. Only if all length scales of the sample are much larger than the equilibration length  $L_{eq}$  a simple scaling with geometry can be found. However, even if a simple geometry dependence is found, the physical meaning of local quantities like  $\rho_{yy}$  or  $\sigma_{xx}$  remains questionable, because these values result in any case from a rather complex interplay of edge and bulk conduction and equilibration between them.

#### References

- [1] Oswald J and Homer A, 2001 Physica E **11**/4 310-322
- [2] Chklovskii D B, Shklovskii B I, Glazmann L I, 1992 Phys. Rev. B **46** 4026
- [3] Wei Y Y, Weiss J, v. Klitzing K, Eberl K, 1998 Phys. Rev. Lett. **81** 1674